An optimized knowledge-based QRS detection algorithm: Evaluation on 11 large-standard ECG databases

Mohamed Elgendi

Department of Computing Science, University of Alberta, Canada

E-mail: moe.elgendi@gmail.com

Abstract

A robust and numerically-efficient method based on a prior knowledge of the ECG event durations is presented. Two optimized event-related moving average filters followed by event-related threshold have been developed to detect QRS complexes. The novelty rises from using window sizes related to the QRS and heartbeat durations. Interestingly, the QRS detector obtained a sensitivity of 99.29% and a positive predictivity of 98.11% over the first lead of the validation databases (11 databases with a total of 1,179,812 beats). When applied to the well-known MIT-BIH Arrhythmia Database a sensitivity of 99.78% and a positive predictivity of 99.87% were attained. Moreover, the speed of the detector is faster than previously published algorithms, and it takes about 2.2 seconds to process 130-minute ECG recordings.

Keywords: two-moving averages, electrocardiogram, QRS detection, ECG analysis, R peak detection, telemedicine, mobile phone

Introduction

According to the World Health Organization, cardiovascular diseases (CVDs) are the number one cause of death worldwide [1]. An estimated 17.3 million people died from CVDs in 2008, representing 30 percent of all global deaths [1].

Recently, medical researchers have placed significant importance on cardiac health research. This has produced a strong focus on preventative, medicinal and technological advances. One such research pathway is leading researchers toward improving the conventional cardiovascular-diagnosis technologies used in hospitals/clinics/home.

The most commonly performed cardiac test is ECG as it is a useful screening tool for a variety of cardiac abnormalities, and is simple, risk-free and inexpensive [2]. The advances in technology have significantly changed to the way we collect, store and diagnose ECG signals, especially regarding the use of mobile phones to replicate these processes [3,4,5].

Moreover, there are some attempts to provide phone applications that analyze ECG signals collected wirelessly via Bluetooth protocol [6,7,8] and Zigbee radio protocol [9]. Mobile telemedicine systems use mobile phones/PDAs to just collect the ECG data—wirelessly or wired—and send them to a central monitoring station using GSM or Internet for further analysis [10,11].

There is no doubt that the essential quality for any algorithm used for real-time analysis is its simplicity (numerical efficiency). The simpler the algorithm, the faster it is in processing large databases [12,13], and less power it consumes on battery driven

devices [9,14,15]. Moreover, a simple algorithm also offers low cost of hardware implementation in both power and size for body sensor networks [16].

Therefore the main goal of this study is to produce a robust and numerically-efficient QRS detection algorithm, with theoretical justification for its parameters choice, tested over 11 large-standard datasets with different sampling frequencies, recording lengths, and noise. Moreover, this study seeks to compare the various QRS detection methods against the developed QRS detection on standard databases.

Furthermore, the theoretical basis of the well-known Pan-Tompkins algorithm [17] will be analyzed and evaluated against the proposed algorithm.

In addition, the instance of failures will be discussed and the processing time of the proposed algorithm will be elaborated on.

Materials and Methods

Data

Several standard ECG databases are available for the evaluation of QRS detection algorithms for ECG signals. The use of one database to test the algorithm can lead to over-tuning problems. This means that the developed algorithm can work perfectly in one database with a specific sampling frequency, recording length and noise. Thus 11 different ECG databases, available on PhyisoNet [18], have been used in this research to evaluate the proposed algorithm. In particular, Lead I from each record is used without excluding any measurement.

These databases contain annotated files for R peaks, which can produce comparable results. They contain a large number of signals representative of a large variety of ECGs, as well as signals that are rarely observed and clinically important.

MIT−BIH Arrhythmia Database

The MIT−BIH Arrhythmia Database [19] is widely used to evaluate QRS detection algorithms. It includes different shapes of QRS complexes and noise, which makes it the most suitable database to test the robustness of the developed ECG algorithms.

The MIT−BIH Arrhythmia Database contains 48 ECG recordings with a total of 109,984 beats. These 30-minute recordings were sampled at 360 Hz.

QT Database

The QT Database [20] contains 105 records (111,201 beats) of 15-minute recording. The records were primarily chosen from among existing ECG databases, including the MIT−BIH Arrhythmia Database, the European Society of Cardiology ST-T Database and several other ECG databases collected at Boston's Beth Israel Deaconess Medical Center. The ECG records were chosen to represent a variety of QRS and ST-T morphologies. All records were sampled at 250 Hz. Those that were not originally sampled at that rate have been converted.

T Wave Alternans Database

The T-Wave Alternans (TWA) Database [21] contains 100 records (19,003 beats) of 120 seconds each, recorded with a 500 Hz sampling frequency. The subjects include patients with myocardial infarctions, transient ischemia, ventricular tachyarrhythmias and other risk factors for sudden cardiac death. It also includes healthy controls and synthetic cases with calibrated amounts of TWA, which is a periodic beat-to-beat variation in the amplitude or shape of the T wave in ECG signals.

Intracardiac Atrial Fibrillation Database

The Intracardiac Atrial Fibrillation (IAF) Database [18] contains 31 records (6,705 beats) with different durations, sampled at 1 kHz. This collection of high-resolution

recordings was obtained from three different placements of the catheter in eight subjects with atrial fibrillation or flutter. In this study Lead I was used.

ST Change Database
The ST Change Database [22] contains 28 records (76,181 beats) recorded with a 360 Hz sampling frequency. The database includes varying lengths of ECG recordings, most of which were recorded during exercise stress tests and exhibit transient ST depression.

Superaventricular Arrhythmia Database
The Supraventricular (SV) Arrhythmia Database [23] contains 78 records (184,744 beats) of 30-minute each, recorded with a 128 Hz sampling frequency. These ECG recordings were chosen to supplement the examples of SV arrhythmias in the MIT−BIH Arrhythmia Database.

Atrial Fibrillation Termination Database
The Atrial Fibrillation Termination (AFT) Database [24] contains 80 records (7,618 beats) of 60-second recording each, recorded with a 128 Hz sampling frequency. Each record exhibits either self-terminating or sustained atrial fibrillation.

Each record is a one-minute segment of atrial fibrillation containing two ECG signals. The segments were extracted from long-term (20- to 24-hour) ECG recordings.

Fantasia Database
The Fantasia Database [25] contains records of 120 minutes each, recorded with a 250 Hz sampling frequency, from 20 young people (21–34 years old) and 20 elderly people (68–85 years old) who were rigorously screened and found to be healthy subjects.

All subjects remained in a resting state in sinus rhythm while watching the movie *Fantasia*. This dataset has 40 records; however, record 'f2y02' is corrupt. Therefore, this record was excluded and the total number of records used was 39 (278,996 beats).

NST Database
The Noise Stress Test (NST) Database [26] contains 12 records (26,370 beats) of 30 minutes each, recorded with a 360 Hz sampling frequency. This dataset contains noise that is typical in ambulatory ECG recordings made using physically active volunteers and standard ECG recorders, leads and electrodes.

ICART Database
The St. Petersburg Institute of Cardiological Technics Arrhythmia (ICART) Database [18] contains 75 records (175,918 beats) of 30 minutes each, with a 257 Hz sampling frequency. The original records were collected from patients undergoing tests for coronary artery disease (17 men and 15 women, aged 18–80; mean age: 58). No patients had pacemakers; most had ventricular ectopic beats.

Normal Sinus Rhythm Database
The Normal Sinus Rhythm database (NSR) [18] includes 18 long-term ECG recordings of subjects—total of 183,092 beats— who were referred to the Arrhythmia Laboratory at Boston's Beth Israel Hospital (now the Beth Israel Deaconess Medical Center), recorded with a 128 Hz sampling frequency. Subjects included in this database were found to have had no significant arrhythmias; they include five men (aged 26–45) and 13 women (aged 20–50).

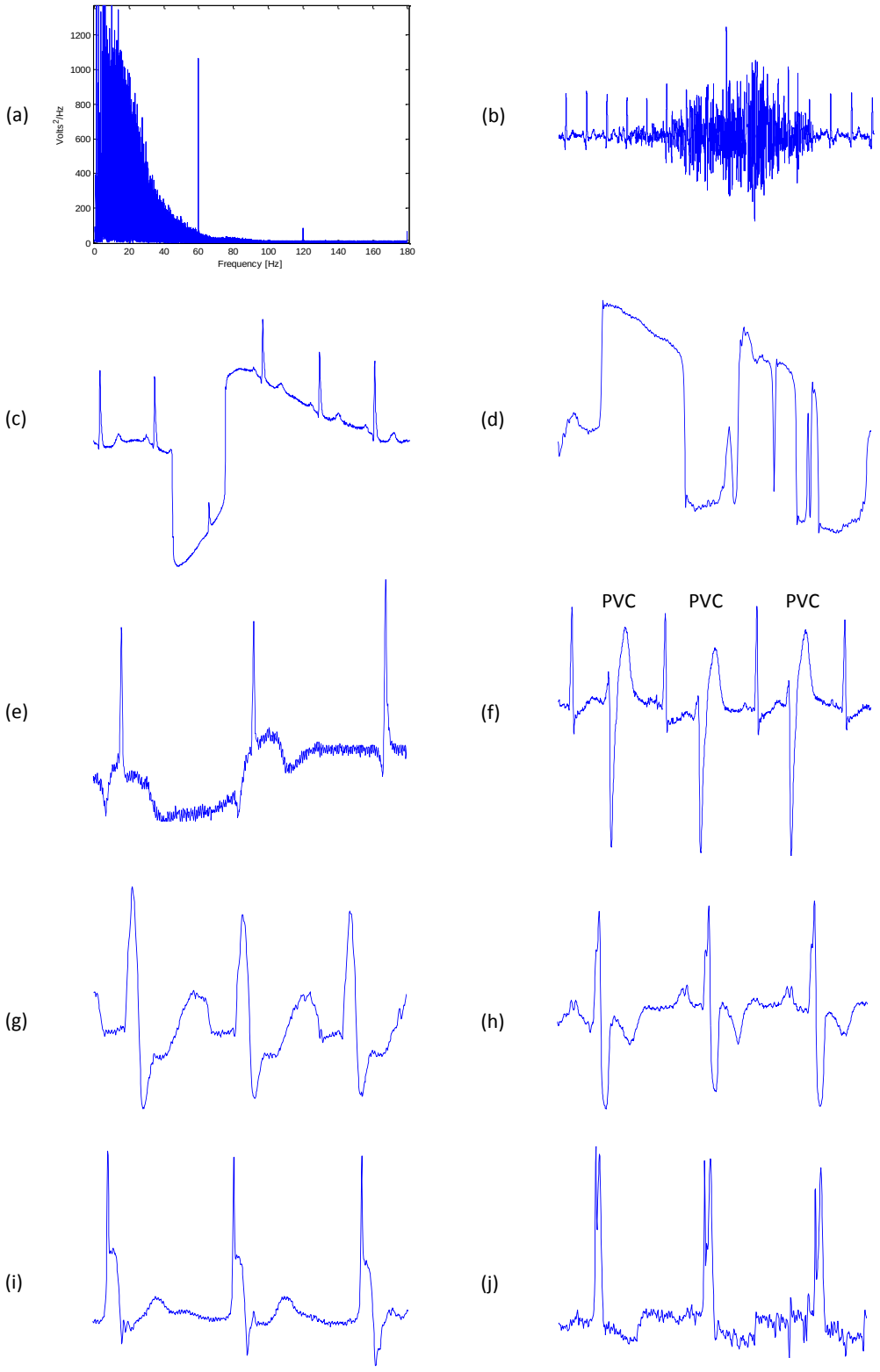

Figure 1 Challenges in detecting QRS in ECG signals. (a) Mains electricity noise: the spectrum illustrates peaks at the fundamental frequency of 60 Hz as well as the second and third harmonics at 120 Hz and 180 Hz, caused by stray magnetic fields causing the enclosure and accessories to vibrate (b) High frequency noise caused by coughing (c) Large movement of the chest (d) Isolated QRS-like artifacts (e) Nodal (junctional) escape beats affected by baseline wandering (f) Premature Ventricular Contractions (g) Left bundle branch block (h) Right bundle branch block.(i) Paced beat (j) Fusion of paced and normal beat

Challenges in ECG

ECG signals can be contaminated with several types of noise and arrhythmias, which may affect the accuracy of the main events detection and overall diagnosis. The challenges could be physiological, caused by the instrumentation used or the experiment's environment. Various types of noise and arrhythmic QRS that corrupt the ECG, which will affect the accuracy of R peaks detection, are shown in Figure 1.

The ECG databases used in this study were collected in the United States (US). Therefore, they contain a frequency component of 60 Hz. The periodic interference is clearly displayed as a spike in Figure 1(a), not only at its fundamental frequency of 60 Hz, but also on its harmonics (e.g. 120 Hz, 180 Hz). Its amplitude can be up to 50% of the peak-to-peak ECG amplitude [27].

Moreover, the databases contain high frequency noise (or muscle noise) as shown in Figure 1(b) and low frequency noise as shown in Figures 1(c,d,e).

Some beats do not have P waves as in the junctional escape beats [28] shown in Figure 1(e). And, some QRS complexes are inverted as the three beats shown in Figure 1(f), which indicate premature ventricular contractions.

Left bundle branch block (LBBB) generates a notched QRS as shown in Figure 1(g), while right bundle branch block (RBBB) generates biphasic QRS complexes and inverted T waves, as shown in Figure 1(h).

The paced ECG complex has two main features [28]: 1) a narrow 'pacing spike,' which reflects the energy delivered from the pacemaker (cf. Figure 1(i)); and 2) the P wave/QRS complex immediately following the 'pacing spike,' as shown in Figure 1(i). The paced P wave atrial has a spike followed by a P wave and a normal QRS complex, where the paced QRS ventricular has a spike followed by a bizarre QRS complex (cf. Figure 1(i)). Moreover, fusion of paced and normal beats is shown in Figure 1(j).

Methodology

In this section, a new, knowledge-based, numerically efficient and robust algorithm is proposed to detect QRS complexes in ECG signals based on two event-related moving-average filters. The structure of the proposed algorithm is shown in Figure 2.

It is clear that the knowledge base is supporting the decision making of both stages: generating blocks of interest and thresholding.

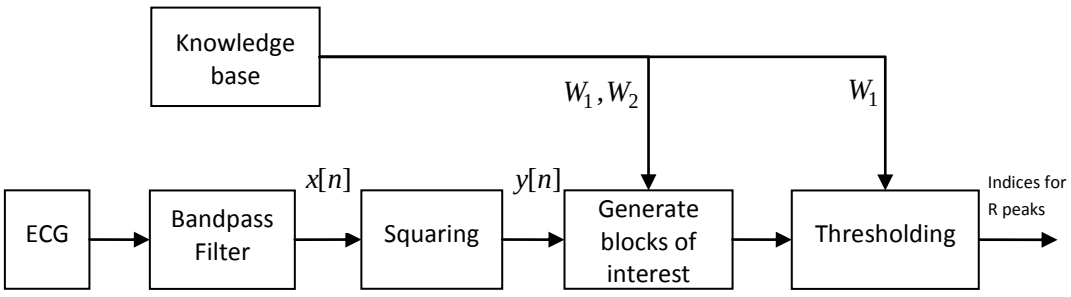

Figure 2 Flowchart of the knowledge-based QRS detection algorithm. The algorithm consists of three stages: pre-processing (bandpass filter and squaring), feature extraction (generating blocks of interest based on prior knowledge) and thresholding (based on prior knowledge).

Knowledge-base Analysis

It is expected that developing a detector that depends on prior knowledge of the ECG features will improve the overall performance and detection accuracy.

Clifford *et al*. [29] provided a mini knowledge-base of the normal limits for the main events within the EGG, for a healthy male adult at 60 beats per minute (bpm), shown in Table 1.

Table 1 ECG Features and Their Normal Values in Sinus Rhythm. The ECG features (P, QRS and T waves) measured from a healthy male adult at a heart rate of 60 beats per minute (bpm). It is critical for the new developed algorithms to have an estimate for the event duration before processing the ECG signal. These durations will play a role in determining the window size of the moving averages and threshold values.

Feature	Normal Value	Normal Limit	Normal duration for sampling frequency of 360 Hz
P width	110 ms	±20ms	33−47 samples
PQ/PR interval	160 ms	±40ms	43−72 samples
QRS width	100 ms	±20ms	29−43 samples

The prior knowledge of the duration of the main events of the ECG signals can assist the feature extraction and support the decision making of the algorithm. For example, in this work, knowing that the QRS duration in a normal-healthy subject varies from 29 to 43 samples, for sampling frequency (SF) of 360 Hz, determines W_1 in generating blocks of interest and thresholding (cf. Figure 2).

Similarly, the average heartbeat duration will determine W_2 in generating blocks of interest. An average value for heartbeat duration is one second in healthy subjects, which means 360 samples (for sampling frequency of 360 Hz).

At this stage, W_1 and W_2 can be initialized by the prior knowledge that has been mentioned above. However, these durations will vary from person to person. Therefore, the exact value for W_1 (QRS duration) and W_2 (one beat duration) will be determined after a brute force search, which will be discussed later in the parameter optimization section.

Bandpass Filter

Morphologies of normal and abnormal QRS complexes differ widely. The ECG signal is often corrupted by noise from many sources, which have been discussed above. Therefore, band-pass filtering is an essential first step for nearly all QRS detection algorithms. The purpose of band-pass filtering is to remove the baseline wander and high frequencies that do not contribute to QRS complex detection.

A band-pass filter will be used, typically a bidirectional Butterworth implementation [30]. It offers good transition-band characteristics at low coefficient orders, which makes it efficient to implement [30]. Thakor et al. [31] and Chen and Chen [32] scored high accuracy using a third-order Butterworth filter with a passband of F1−F2 Hz to remove baseline wander and high frequencies, and to suppress the P and T waves and maximize the QRS area, where F1 is the starting frequency and F2 is the stopping frequency. The effect of the Butterworth filter can be seen in Figure 3 (b). However, a rigorous optimization over the passband, to find the optimal frequency band, will be discussed in the parameter optimization section.

Squaring Function

The signal is squared point by point, to enhance large values and boost high-frequency components, using the following equation:

$$y[n] = (x[n])^2 . \tag{1}$$

The impact of the squaring is shown in Figure 3 (c).

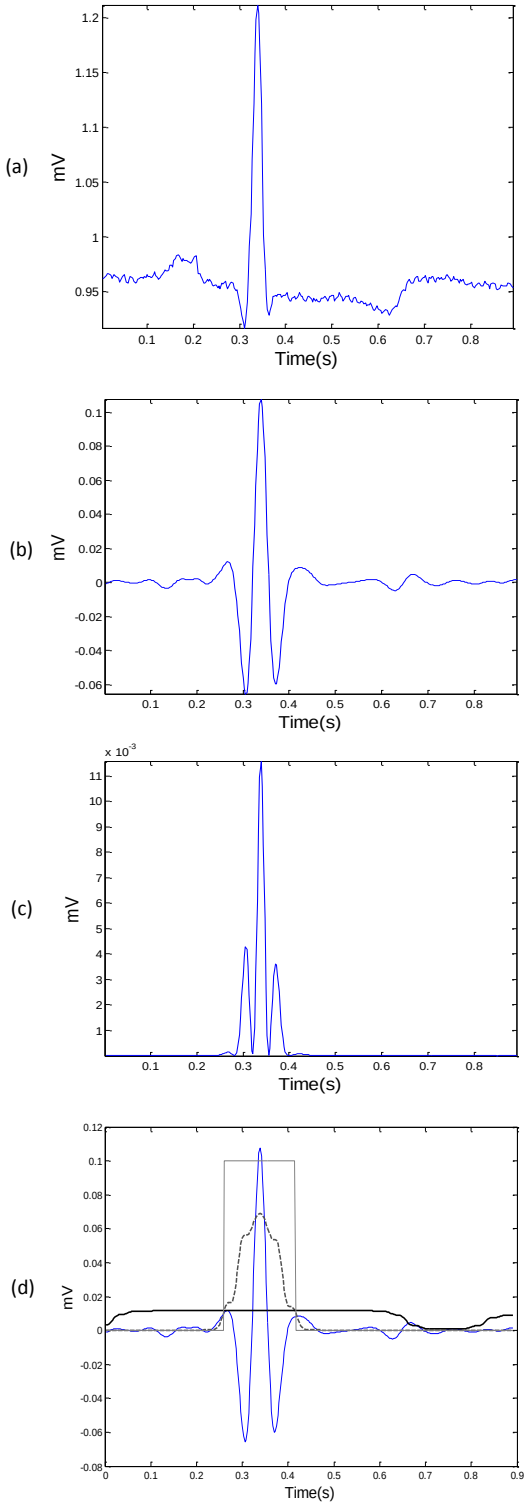

Figure 3 Demonstrating the effectiveness of using two moving averages to detect QRS complex (a) one beat ECG signal (b) filtered one-beat ECG signal with Butterworth band-pass filter (c) squaring the filtered signal (d) generating blocks of interest after using two event-related moving averages: The dotted line is the MA_{QRS} and the solid line is the $MA_{OneBeat}$. The R peak within the block of interest is then detected after applying the event-related threshold.

.

Generating Blocks of Interest

Blocks of interest will be generated using two event-related moving averages. The first moving average MA_{QRS} is used to extract the QRS features while the second-moving average MA_{Beat} extracts the QRS's beat. Then, an event-related threshold will be applied to the generated blocks to distinguish the blocks that contain R peaks from the blocks that include noise.

QRS Moving Average

The purpose of the QRS moving (MA_{QRS}) average is to smooth out multiple peaks corresponding to QRS complex intervals in order to emphasize and extract the QRS area:

$$MA_{QRS}[n] = \frac{1}{W_1}(y[n-(W_1-1)/2] + ... + y[n]... + y[n+(W_1-1)/2]) \qquad (2)$$

where W_1 is the approximate duration of QRS complex, rounded to the nearest odd integer, and n is the number of data points.

Based on the knowledge-base analysis section, the QRS duration W_1 varies from 29 to 43 samples (for sampling frequency of 360 Hz). Therefore a rigorous optimization to find the optimal W_1 will be discussed in the parameter optimization section.

One-Heartbeat Moving Average

The purpose of one-beat moving average ($MA_{OneBeat}$) is similar to MA_{QRS} but emphasizes the QRS's beat to be used as a threshold for the first moving average (MA_{QRS}):

$$MA_{OneBeat}[n] = \frac{1}{W_1}(y[n-(W_1-1)/2] + ... + y[n]... + y[n+(W_1-1)/2]) \qquad (3)$$

where W_2 is the approximate duration of a heartbeat, rounded to the nearest odd integer, and n is the number of data points.

Based on the knowledge-base analysis section, heartbeat duration W_2 is about 360 samples (for sampling frequency of 360 Hz); however it varies from person to person. Therefore a rigorous optimization to find the optimal W_1 will be discussed in the parameter optimization section.

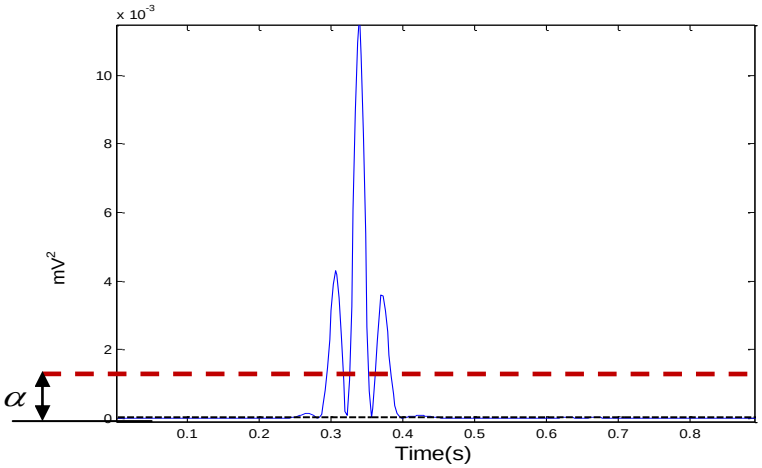

Figure 4 Demonstrating the statistical threshold. The squared one-beat ECG signal (z) which is shown in Figure 3 (c), where the dashed line represents the offset caused by α .

The blocks of interest are generated based on the two moving averages discussed above. In other words, applying the second-moving average $MA_{OneBeat}$ as a threshold to

the first-moving average MA_{QRS} produces block of interest. However, the use of $MA_{OneBeat}$ without an added offset reduces the detection accuracy because of its sensitivity to low SNR.

As the SNR defined the ratio of the mean signal of a region of interest to its standard deviation [33], which means if the statistical mean of the signal is increased, the SNR becomes higher. This leads to introducing an offset based on the statistical mean of the signal as

$$\alpha = \beta \bar{z} \tag{4}$$

where β is the fraction of the $\bar{z}$ signal that needs to be removed, $\bar{z}$ is the statistical mean of the squared ECG signal z, as illustrated in Figure 4 and α is an offset for the threshold $MA_{OneBeat}$ signal.

In short, to increase the accuracy of detecting QRS complexes in noisy ECG signals, the dynamic threshold value $THR1$ is calculated by offsetting the $MA_{OneBeat}$ signal with α, as follows:

$$THR1 = MA_{OneBeat}[n] + \alpha \tag{5}$$

The blocks of interest will then be generated by comparing the MA_{QRS} signal with $THR1$. If a block is higher than $THR1$, it is classified as a block of interest containing ECG features (P, QRS or T) and noise; otherwise, as shown in lines 10-16 in Figure 5.

By this stage, blocks of interest have been generated, *Blocks*[*n*]. Therefore, the next step is to reject the blocks that result from noise. The rejection should be related to the anticipated block width.

Thresholding

Here, the undesired blocks are rejected by using the new *THR2* threshold to reject the blocks that contain P and T waves and noise. By applying the *THR2* threshold, the accepted blocks will contain only QRS complexes:

$$THR2 = W_1 \tag{6}$$

As discussed, the threshold *THR2* equals W_1, which corresponds to the anticipated healthy QRS width. If the block width equals the window size W_1, then the block contains a QRS complex. However, the QRS duration varies in arrhythmia ECG signal durations. Therefore, the condition is set to capture both average (healthy beats) and wide (arrhythmia beats) QRS complex durations.

Therefore, if a block width is greater than or equal to W_1, it is classified as a QRS complex. If not, the block is classified as a P wave, T wave or noise.

Detecting R Peaks

The last stage is finding the maximum absolute value within each block, which is considered the R peak.

Algorithm 1 QRS Detector

```
Create function QRS_Detector(F1,F2,W1,W2,β)

    Filtered=Bandpass(ECG, F1-F2)
    Sq_Filtered=Square(Filtered
    MA_QRS=MA(Sq_Filtered, W1)
    MA_OneBeat=MA(Sq_Filtered, W2)
    z= mean(Sq_Filtered)
    α= βz+ MA_OneBeat
    THR1=MA_OneBeat + α
    for n=1 to length(MA_QRS) do
        if  MA_QRS[n]>THR1  Then
            BlocksOfInterest[n]=0.1
        Else
            BlocksOfInterest[n]=0
        End if
    END for
    Blocks ← onset and offset from BlocksOfInterest
    Set BlockSize = W1
    for j=1 to number of blocks do
        if  width(Blocks[j])>= BlockSize Then
            R_Peak ← max value with this block
        Else
            Ignore this block
        End if
    END for

End function
```

Figure 5 Pseudocode for the knowledge-based QRS detector function. The function has five inputs: F1, F2, W_1, W_2 and β. The band-pass filter will be determined by the frequency band F1−F2 Hz, while W_1 and W_2 are the window sizes of the two moving averages MA_1 and MA_2, respectively. However, β will be used to calculate the event-related threshold α.

Parameters Optimization

The function of the QRS detector, which is presented in Figure 5, has five inputs: the frequency band (F1−F2), event-related durations W_1 and W_2 and the offset (β). Any change in these parameters will affect the overall performance of the proposed algorithm. These parameters are interrelated and cannot be optimized in isolation. A rigorous optimization, brute-force search based on the knowledge-base information, over all parameters is conducted, as shown in Figure 6. It is time-consuming, as the complexity of the algorithm is $O((MaxF1\text{-}F1) \times (MaxF2\text{-}F2) \times (MaxW_1\text{-}W_1) \times (MaxW_2\text{-}W_2) \times Max\beta)$, but it is required before making any claims.

Algorithm 2 Detector Optimizer

```
Initialize
MaxF1=10,MaxF2=25,MaxW1=40,MaxW2=250,Maxβ=0.1
for F1=1 to MaxF1 with step=1 do
    for F2=F1+10 to MaxF2 with step=1 do
        for W1=20 to MaxW1 with step=5 do
            for W2=200 to MaxW2 with step=10 do
                for β=0 to Maxβ with step=0.01 do
                 R_Peaks=QRS_Detector(F1,F2,W1,W2,β)
                 Calculate SE,+P
                END for
            END for
        END for
    END for
END for
```

Figure 6 Pseudocode for the brute-force optimizer. The optimizer is initialized with *MaxF1*=10 Hz, *MaxF2*=25 Hz, *MaxW1*=40 samples, *MaxW2*=250 samples, *Maxβ*=0.1. Systematically, this exhaustive search enumerates all possible combinations for the solution and checks whether each combination provides an optimal detector based on *SE* and *+P*.

Table 2 A rigorous optimization of all parameters of the algorithm: frequency band, W_1, W_2 and the offset. All possible combinations of parameters (37,950 iterations) have been investigated and sorted into descending order according to their overall accuracy. The database used is the MIT−BIH Arrhythmia Database. The overall accuracy is the average value of SE and +P.

Combination	Frequency Band	*W1* (samples)	W_2 (samples)	Offset (%)	SE (%)	+P (%)	Overall Accuracy (%)
1	8-20 Hz	35	220	8	99.78	99.87	99.83
2	8-19 Hz	40	220	10	99.76	99.89	99.83
3	9-19 Hz	40	220	9	99.77	99.89	99.83
4	8-20 Hz	40	220	8	99.79	99.87	99.83
5	8-20 Hz	35	220	9	99.77	99.89	99.83
6	8-19 Hz	35	220	9	99.76	99.89	99.83
7	8-21 Hz	40	220	8	99.79	99.87	99.83
8	8-21 Hz	40	230	9	99.77	99.89	99.83
9	9-19 Hz	35	230	9	99.76	99.89	99.83
10	8-21 Hz	35	220	9	99.77	99.88	99.82
11	8-21 Hz	35	210	9	99.78	99.87	99.82
12	8-18 Hz	40	220	10	99.75	99.90	99.82
13	8-21 Hz	40	220	9	99.77	99.88	99.82
14	8-18 Hz	35	220	9	99.76	99.89	99.82
15	8-21 Hz	35	220	8	99.78	99.86	99.82
16	8-22 Hz	35	220	9	99.77	99.88	99.82
17	8-22 Hz	35	220	10	99.75	99.89	99.82
.	.	.	.	.	.	.	.
.	.	.	.	.	.	.	.
37947	1-26 Hz	20	200	7	33.713	93.869	63.791
37948	1-26 Hz	20	200	8	33.263	93.907	63.585
37949	1-26 Hz	20	200	9	32.803	93.962	63.383
37950	1-26 Hz	20	200	10	32.371	94.127	63.249

Results

Performance of QRS detection algorithm is typically done using two statistical measures: SE=TP/(TP+FN) and +P=TP/(TP+FP), where TP is the number of true positives (QRS complexes detected as QRS complexes), FN is the number of false negatives (QRS complexes have not been detected as QRS complexes) and FP is the number of false positives (non-QRS complexes detected as QRS complexes). The sensitivity (SE) reports the percentage of true beats that were correctly detected by the algorithm. The positive predictivity (+P) reports the percentage of beat detections that were true beats.

It can be seen from Figure 6, the optimizations of the beat detector's spectral window for lower frequency varied from 1−10 Hz, with the higher frequency up to 26 Hz. All combinations of the frequency band 1−26 Hz have been explored to include all frequency bands that have been recommended in literature such as 8−20 Hz [12], 5−15 Hz [31,32] and 5−11 Hz [17]. The window size of the MA_{QRS} (W_1) ranged from 55 to 111 ms, whereas the window size of the $MA_{OneBeat}$ (W_2) changed from 555 ms to 694 ms as discussed in the knowledge-base analysis section. However, the offset tested over the range 0−10% of the mean value of the squared filtered ECG signal.

The database used in the optimization process is MIT-BIH Arrhythmia Database because it contains: abnormal rhythms, different QRS morphologies, and low SNR signals, as described in challenges in the ECG section. The total number of beats in MIT-BIH Arrhythmia Database is 109,984 beats, and there are 48 records. As discussed, several publications have listed the use of all files in the database, excluding just the paced patients, segments and certain beats. However, in the optimization process all records have been used without excluding any beat.

After the rigorous optimization, all parameters combinations were sorted in a descending according order according to the overall accuracy, as shown in Table 2; thus the first combination provides the optimal solution.

The highest overall-accuracy score is 99.83% (cf. Table 2), therefore the optimal frequency range for QRS detection in the MIT-BIH Arrhythmia Database is 8−20 Hz, as proposed by Benitez et al. [12]. Moreover, the optimal values for the moving averages and offset are W_1=97 ms (35 samples for SF=360 Hz) and W_2=611 ms (220 samples for SF=360 Hz), and $\beta = 8$.

Now, an optimal QRS detector is accomplished over the MIT-BIH Arrhythmia Database. Then, we can test this detector on other datasets 'straight out of the box' without any tuning. By doing that, the robustness of the algorithm is examined as the algorithm will be applied to different databases with different sampling frequencies and the ECG signals collected by different doctors in dissimilar conditions.

Table 3 shows the performance of the QRS detection algorithm on 11 databases. Moreover, it summarizes the performances across these databases and compares them to other reported results. Because the algorithm has not been re-tuned over any databases, the results are promising and the algorithm is able to detect R peaks over different databases, sampling frequencies, types of arrhythmias and types of noise.

The number of beats used to calculate these performance parameters is indicated in the second column of Table 3.

Hamilton and Tompkins implemented their QRS detection algorithm in 1986. They scored 99.69% SE and 99.77% +P over 109,267 beats from MIT-BIH Database (cf. Table 3). When Arzeno et al. [12] applied Hamilton-Tompkins's algorithm over a slightly larger number of beats, 109,504 beats, the detector performance went down slightly, scoring a SE of 99.68% and a +P of 99.63%.

Table 3 QRS detection performance comparison. Several algorithms have been compared using the MIT−BIH Database (N/R: NOT REPORTED).

	No. of beats	No. of beats	SE(percent)	+P(percent)
MITDB	This work	109984	99.78	99.87
	Pan and Tompkins [17]	115353	99.76	99.56
	Chouhan (Method I)	44677	87.90	97.60
	Improved Chouhan (Method II)	44677	97.5	99.90
	Adnane et al. [34]	109487	99.77	99.64
	Ghaffari [35]	109837	99.91	99.72
	Benitez et al. [12]	109257	99.13	99.31
	Modified Benitez et al. [12]	109517	99.29	99.24
	Hamilton and Tompkins [12]	109504	99.68	99.63
	Modified Hamilton-Tompkins [12]	109436	99.57	99.58
	Second derivative of Hamilton-Tompkins [12]	108228	98.08	99.18
	Huabin and Jiankang [36]	N/R	98.68	99.59
	Fard et al. (HCW) [37]	24000	99.79	99.89
	Fard et al. (CFBSW) [37]	24000	99.29	99.89
	Fard et al. (CNW) [37]	24000	99.49	99.29
	Darrington [38]	109487	99.06	99.20
	Chen et al. [39]	102654	99.55	99.49
	Martinez et al. [40]	109428	99.80	99.86
	Hamilton [41]	N/R	99.80	99.80
	Lee et al. [42]	109481	99.69	99.88
	Afonso et al. [43]	90909	99.59	99.56
	Li et al. [44]	104182	99.89	99.94
	Hamilton and Tompkins [45]	109267	99.69	99.77
QTDB	This work	111201	99.99	99.67
	Martinez et al. [40]	86892	99.92	99.88
	Aristotle [40]	86892	97.20	99.46
NSTDB	This work	26370	95.39	90.25
	Benitez et al. [46]	N/A	93.48	90.60
TWADB	This work	19003	98.88	99.12
STDB	This work	76181	99.92	99.70
SVDB	This work	184744	99.96	99.80
IAFDB	This work	6705	99.59	94.11
NSRDB	This work	183092	99.99	99.96
AFTDB	This work	7618	99.72	99.74
FANTASIA DB	This work	278996	99.98	99.87
INCART DB	This work	175918	99.03	97.09

It is worth noting that Li et al. [44] scored higher performance, a sensitivity of 99.89% and a specificity of 99.94%, than the proposed algorithm. This is because Li et al. excluded files 214 and 215 from the MIT-BIH Database, and therefore their algorithm is not superior in terms of performance. However, their algorithm was based on wavelets feature extraction and singularity for classification, which is considered numerically inefficient.

Moreover, the algorithm developed by Ghaffari et al. [44] scored a sensitivity of 99.91% and a specificity of 99.72% over 109,837 beats (not all beats); their algorithm was based on wavelets feature extraction and thresholds for classification, which is also considered numerically inefficient.

Conversely, the proposed knowledge-based algorithm presents a clear advantage over the previously reported algorithms in terms of performance (large number of databases) and numerical efficiency. This was clear with MIT-BIH Arrhythmia Database, as discussed above. Besides, the QTDB where the detector scored an SE of 99.67% and a +P of 100%, over 111,193 beats, without excluding any beat as Martinez et al. [40] and Aristotle [40] did. Furthermore, the overall performance of the detector on the NSTDB was higher than Benitez et al. [46], with clear mentioning of the number of beats used, specifically 26,370 beats.

Discussion

After describing the detector and its results on different datasets, perhaps further elaboration on the detector's performance is required. However, comparing the performance of the proposed algorithm with previously published algorithms is difficult. This is because of not testing the developed algorithms on the same data, in particular the same beats.

By excluding number of beats and/or certain records, the performance of any detector will score higher detection rates. Here are a few examples to clarify the idea:

- Xue et al.[47] reported sensitivities of 99.84% and 99.09 % and positive predictivity of 99.61% and 98.59 % based on just two records, number 105 and 108 from the MIT-BIH Arrhythmia Database [48].
- Wavelet transforms have been used for QRS detection by Li et al. [49]. They reported 0.15% false detections based on 46 files from the MIT-BIH Arrhythmia Database [48], excluding files 214 and 215.
- Moraes et al. [50] logically combined two different algorithms working in parallel, the first adopted from the work of Englese and Zeelenberg [51], the second based on Pan and Tompkins [17] and Ligtenberg and Kunt [52]. Moraes et al. reported sensitivity of 99.22% and specificity of 99.73% after having excluded records of patients with pacemakers. However, they also excluded recordings 108, 200, 201 and 203, from the MIT-BIH Arrhythmia Database.
- Continuous Spline Wavelet Transform using local maxima of the Continuous Wavelet Transform at different scales have been used by Alvarado et al. They reported sensitivity of 99.87% and positive predictivity of 99.82 % after using just nine files out of 48 files from MIT-BIH Arrhythmia Database [53].
- Zhang et al. [54] have used the Continuous Wavelet Transform using fixed thresholds. They reported accuracy of 99.5% after using just eight files out of 48 files from MIT-BIH Arrhythmia Database.

Most of the proposed algorithms were tested on one dataset, the MIT-BIH Arrhythmia Database. The authors exclude some records from the used database to improve the overall accuracy. Here is an example based on the proposed detector, if records 108 and 207 are excluded from this study, the proposed detector scores SE of 99.9% and +P of 99.95%, which does not reflect the real performance of the algorithm. Therefore, the author urges the readers, researchers and biomedical-signal-analysis community of using the standard databases with excluding any record or beat.

Now, after discussing the misleading conclusions based on data elimination, the performance of the proposed detector can be discussed technically. The main technical aspects of any QRS detector are: frequency-band choice, window-size and threshold choices, instances of failure and processing time.

Frequency-Band Choice

In literature, the QRS frequency band has been used without actually identifying the optimum QRS frequency range for the detection of the QRS complexes. Different researchers used different passbands; for example, Thakor et al. [31] proposed an estimate of QRS complex spectra and suggested that the passband that maximizes the QRS energy is approximately 5−15 Hz.

Pan and Tompkins [17] used cascaded low-pass and high-pass filters to achieve a passband of about 5−11 Hz. Li et al. [44] used a quadratic spline wavelet with compact support and one vanishing moment. Their conclusion was that most QRS complex energies are at the scale of 2^4, that is, its Fourier transform frequency range lies between 4 and 13.5Hz. Sahambi et al. [55] used the first derivative of a Gaussian

smoothing wavelet and found that most QRS complex energies are at the scales of 2^3 and 2^4, with corresponding frequency ranges between 4.1 Hz and 33.1 Hz.

Benitez et al. [46] developed a QRS detection algorithm using the properties of the Hilbert transform with band stop frequencies at 8 and 20 Hz in order to remove muscular noise and maximize the QRS complex, respectively. Moraes et al. [50] combined two improved QRS detectors using a band-pass filter between 9 and 30 Hz.

Chen and Chen [32] introduced a QRS detection algorithm based on real-time moving averages and assumed the QRS frequencies were concentrated at approximately 5−15 Hz. Mahmoodabadi et al. [56] used Daubechies2 to detect QRS complex using scales of 2^3–2^5, which covers the frequency range of 2.2−33.3 Hz.

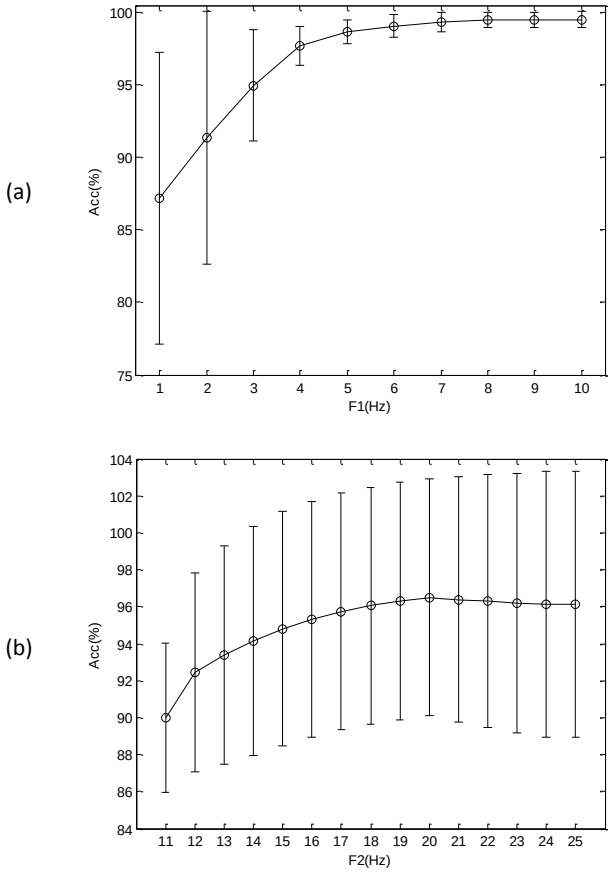

Figure 7 Influence of frequency bands on the overall accuracy based on the brute-force optimization. (a) Frequency band starts at value within 1−10 Hz. (b) Frequency band stops at value within 11−25 Hz, where the circle is the statistical mean and the bar is the standard deviation.

Most of these authors evaluated their algorithms using the MIT−BIH database and determined the frequency bands experimentally, without justifying their choice. Thus, the proposed detector provides an optimal frequency band for detecting QRS complexes, which is 8−20 Hz, justified by a rigorous brute-force optimization, as elaborated in the parameter optimization section.

Moreover, Figure 7 shows the influence of a certain frequency band on the overall accuracy. It is clear that F1 scores consistent results above 5 Hz, as shown in Figure 7(a). Thus, in designing a band-pass filter, the starting frequency should lie within 5−10 Hz.

Regarding the stopping frequency, F2, perhaps the optimal choice is 20 Hz, which has highest average and lowest standard deviation; 19 and 21 Hz can still provide relatively high accuracy.

Table 4 Comparison between the proposed QRS detection algorithm and Pan and Tompkins' algorithm.

Step	Proposed Algorithm	Pan and Tompkins [17]
Band-pass Filtering	-Passband: 8-20 Hz -Delay: Zero sample -Implementation: $s[n]=\sum_{k=0}^{N} b_k\, ECG[n-k]-\sum_{k=1}^{N} a_k s[n-k]$ $x[n]=\sum_{k=0}^{N} b_k\, s[n-k]-\sum_{k=1}^{N} a_k x[n-k]$	-Passband: 5-15 Hz -Delay: 16 samples -Implementation: $s[n]=2s[n-1]-s[n-2]+ECG[n]-2ECG[n-6]+ECG[n-12]$ $x[n]=32s[n-16]-(x[n-1]+s[n]-s[n-32])$
Differentiation	N/A	$q[n]=(1/8)(-x[n-2]-2x[n-1]+2x[n+1]+x[n+2])$
Squaring	$y[n]=(x[n])^2$	$y[n]=(q[n])^2$
Integration	$MA_{QRS}[n]=\frac{1}{W_1}(y[n-(W_1-1)/2]+....+y[n]....+y[n+(W_1-1)/2])$ $where \quad W1=97ms*SF$	$MA_{QRS}[n]=\frac{1}{W}(y[n-(W-1)]+y[n-(W-2)]+...+y[n])$ $where \quad W=150ms*SF$
Thresholds used	$MA_{OneBeat}[n]=\frac{1}{W_2}(y[n-(W_2-1)/2]+....+y[n]....+y[n+(W_2-1)/2])$ $where \quad W1=611ms*SF$ $THR1=MA_{OneBeat}[n]+\alpha$ $THR2=W_1$	$SPKI=0.125\ PEAKI+0.875\ SPKI$ $NPKI=0.125\ PEAKI+0.875\ NPKI$ $THRESH\ I1=0.25(SPKI-NPKI)$ $THRESH\ I2=0.5\ THRESH\ I1$ $SPKI=0.25\ PEAKI+0.75\ SPKI$ $SPKF=0.125\ PEAKF+0.875\ SPKF$ $NPKF=0.125\ PEAKF+0.875\ NPKF$ $THRESH\ F1=NPKF+0.25(SPKI-NPI$ $THRESH\ F2=0.5THRESH\ F1$ $SPKF=0.25\ PEAKF+0.75\ SPKF$
Adjusting thresholds to detect arrhythmia		$THRESH\ I1\leftarrow 0.5\ THRESH\ I1$ $THRESH\ F1\leftarrow 0.5\ THRESH\ F1$ $RR\ AVG1=0.125\ (RR_{n-7}+RR_{n-6}+...+RR_$ $RR\ AVG2=0.125\ (RR'_{n-7}+RR'_{n-6}+...+RR'$ $RR\ LOWLIMIT=92\%\ RR\ AVG2$ $RR\ HIGHT\ LIMIT=116\%\ RR\ AVG2$ $RR\ MISSED\ LIMIT=166\%\ RR\ AVG2$ $RR\ AVG2\leftarrow 0.5\ RR\ AVG1$

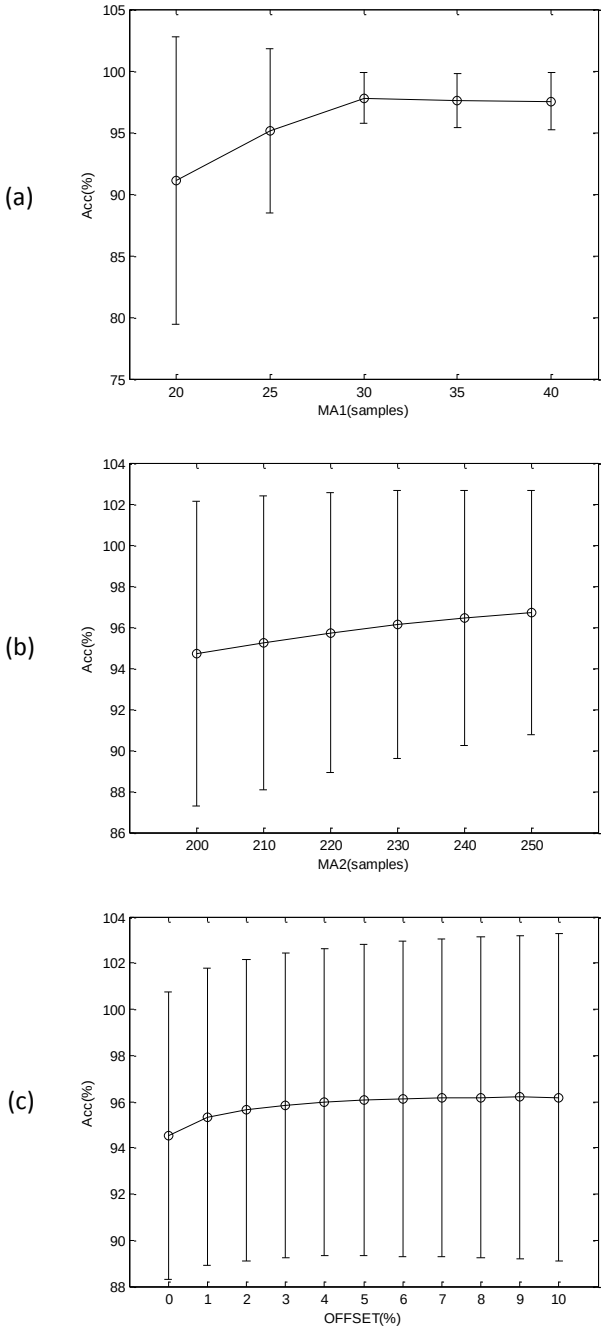

Figure 8 Influence of window sizes and offest on the overall accuracy based on the brute-force optimization. (a) The window size of the MA_{QRS} varies from 20 to 40 samples, for SF=360 Hz. (b) The window size of the $MA_{OneBeat}$ varies from 200 to 250 samples for SF=360 Hz. (c) The offset varies from 0 to 10%, where the circle is the statistical mean and the bar is the standard deviation.

Window-Size and Threshold Choices

Researchers generally used a fixed window size for the moving average that demarcates the QRS complex; for example, a window size of 30 (which is 150 ms) has been used empirically by Pan and Tompkins [17], and it produced good results over the MIT-BIH Arrhythmia Database. However, the window size of the moving average is related to the duration of the QRS complex.

This is not an easy task, as the duration of the QRS complex is genetic-dependent and can be affected by heart rate. It is impractical to take the genetic factor into account, as the correlation between QRS duration and genes is not known.

Perhaps considering the heart rate in detecting R peaks would be a good idea, especially in arrhythmic ECG signals. However, we first need to determine the heart rate accurately, which is the main objective in the first place.

Pan and Tompkins proposed a QRS detection algorithm that adjusts the used thresholds based on the eight most recent beats [17]. The problem here is that the current processed ECG segment will depend on the accuracy of the heart rate determined in the previous segment. A domino effect of errors will occur. Therefore, a new solution is needed that does not depend on genetic information or the recent heart rate.

The proposed detector overcomes these issues by searching for the optimized window sizes for the QRS and heartbeat durations. However, it shares some steps with Pan and Tompkins' algorithm. A comparison is presented in Table 4 to show the main differences and the novelty of the proposed methodology, which is the optimized knowledge-base consideration.

It is clear from Table 4 that the proposed algorithm is far less complex compared to Pan and Tompkins' algorithm. The new algorithm uses an optimized window size for the moving average that demarcates the QRS complex efficiently. Moreover, it eliminates the multiple static thresholds by using a secondary moving average with an optimized window size that demarcates each heartbeat and works as a *data-driven* threshold for the first moving average MA_{QRS}. Thus the proposed detector overcomes the unjustified parameters value and the use of fixed thresholds.

Figure 8 shows the influence of the window sizes of the moving averages and offset on the overall accuracy. It is clear that the optimal window size W_1 for detecting QRS can be 30, 35 or 40 samples (for SF=360 Hz). The optimal window size W_2 for demarcating a heartbeat was hard to determine, as it perhaps can be 220, 230, 240 or 250 samples (for SF=360 Hz). On the other hand, the optimal offset β varies from 2 to 10% (cf. Figure 8(c)).

However, the optimal combination based on the brute-force search was W_1=35 samples≡97 ms, W_2=220 samples≡611 ms and the offset value was β=0.8, as shown in Table 2. However, combinations 2 to 17, in Table 2, provide relatively high accuracy as well.

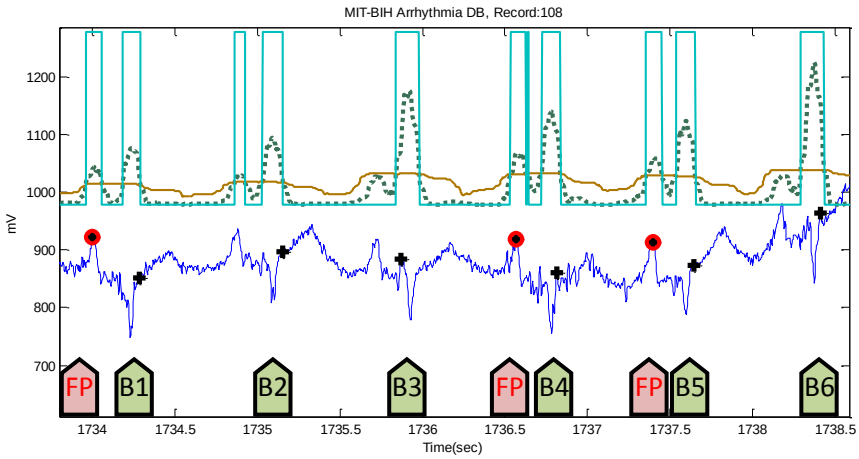

Figure 9 Noisy reversed-polarity QRS complexes in Record 108. The dotted line is the first moving average MA_{QRS} and the solid line is the second moving average $MA_{OneBeat}$. The green arrows point to successful detection, while the pink arrows point to instances of failure. '+' represents a successful detection produced by the proposed algorithm, where the red circle represents *FP*.

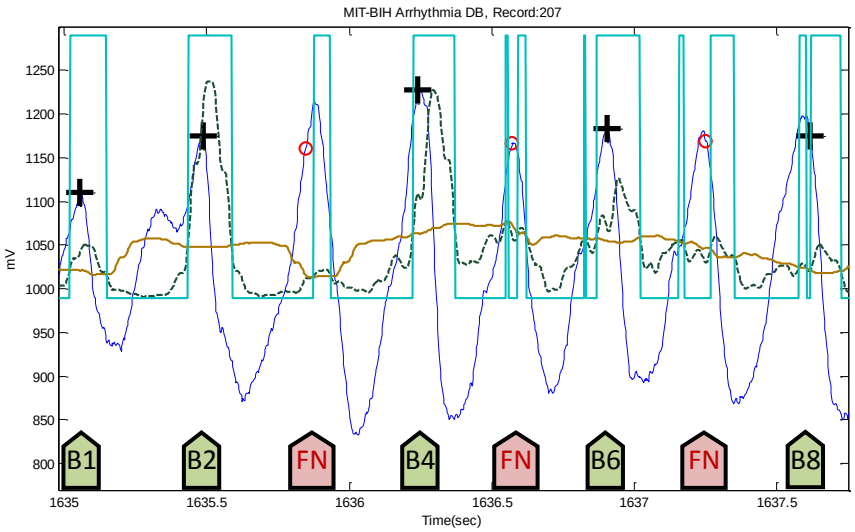

Figure 10 Ventricular flutters in Record 207-MITDB. The dotted line is the first moving average MA_{QRS} and the solid line is the second moving average $MA_{OneBeat}$. The green arrows point to successful detection, while the pink arrows point to instances of failure. '+' represents a successful detection produced by the proposed algorithm, where the red circle represents *FN*.

Instances of Failure

Usually algorithms failed at specific instances within the ECG recordings, which considered either false positives (FPs) or false negatives (FNs).

The proposed algorithm incurred a total of 124 FPs and a total of 247 FNs over the MIT-BIH Arrhythmia Database.

The noisy reversed QRS polarities caused the highest number of FPs in Record 108, as shown in Figure 9, while Record 207 scored the highest number of FNs, precisely 198 FNs, because of the ventricular flutters (cf. Figure 10).

In Figure 9, the two moving averages succeeded in generating blocks of interest that demarcated all QRS complexes, but also demarcated the wide P waves, causing FPs before B1, B4 and B5 shown in Figure 9; and threshold *THR2* could not help in rejecting them. On the other hand, the moving averages could not generate blocks of interest due to the fast rhythm as B3, B5 and B7 show in Figure 10.

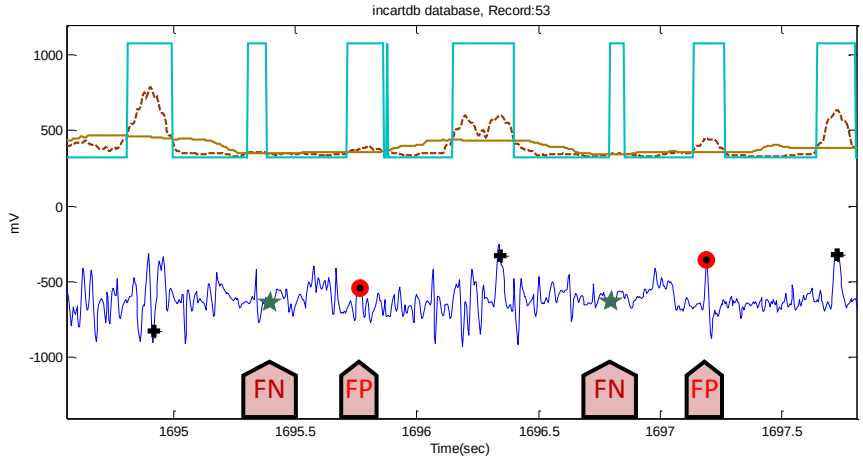

Figure 11 Noisy ECG signals in Record 53-INCARTDB. The dotted line is the first moving average, MA_{QRS} and the solid line is the second moving average $MA_{OneBeat}$. The arrows point to FNs and FPs. '+' represents a successful detection produced by the proposed algorithm, where the red circle represents FP and the green star represents FN.

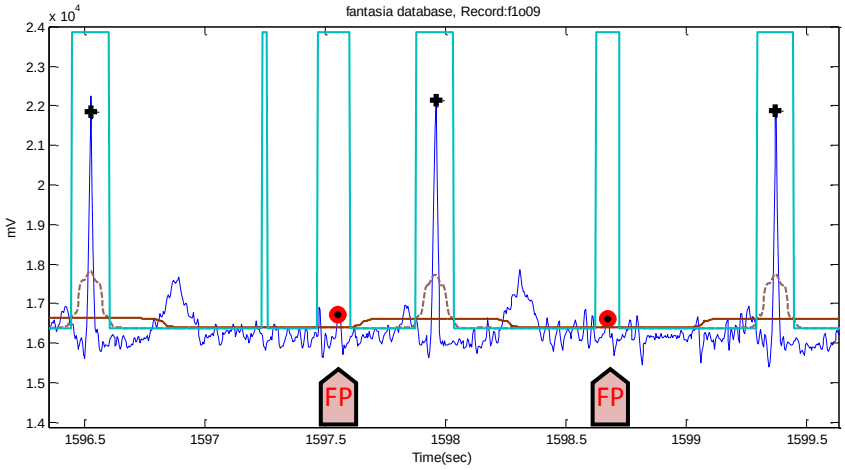

Figure 12 Wide U waves in Record f1o09-FANTASIADB. The dotted line is the first moving average MA_{QRS} and the solid line is the second moving average $MA_{OneBeat}$. The arrows point to FPs. '+' represents a successful detection produced by the proposed algorithm, where the red circle represents FP.

On the INCART database, the algorithm incurred a total of 5197 FPs and 1995 FNs. Because of the very noisy signals, Record 53 had 428 FPs and 104 FNs (cf. Figure 11). It is important to note that the annotations of this database may need revision as the position of the R peaks is very hard to determine, as shown in Figure 11. However, the algorithm runs over the database without any adjustments to the annotated R peaks.

FPs and FNS were 315 and 50 when the algorithm was applied on the FANTASIA database. The highest values of FPs were in record f1o09, where the ECG signals contain wide U waves, as shown in Figure12. Likewise, Record 16272 (in the NSR database) had the most number of FPs, 49 instances out of 63 FPs, because of the existence of U waves.

The algorithm incurred a total of 5197 FPs and 1995 FNs on INCART database. Because of the very noisy signals Record 53 had 428 FPs, and 104 FNs (cf. Figure 11). Important remark, the annotations of this database perhaps needs revision as the position of the R peaks is very hard to determine, as shown in Figure 11. However, the algorithm runs over the database without any adjustments to the annotated R peaks.

Using the AFTDB database, the detector was able to achieve a low number of FPs, and FNs, 17 and 34, correspondingly. Due to the fast rhythm of the atrial fibrillation, the number of FNs was higher than that of the FPs, which is similar to the detector's performance on the MIT-BIH Arrhythmia Database; Figure 10 may clarify the idea of the occurrence of FNs in a fast rhythm.

It is expected that SVDB's performance would have more FNs than FPs, as it contains supraventricular arrhythmias. However, the highest number of FNs registered from Record 848-SVDB due to the rapid heart rhythm. The number of FPs got also higher because of the noisy reversed-polarity QRS beats, as in Record 886 which had the highest number of FPs; exactly 99 of a total of 356.

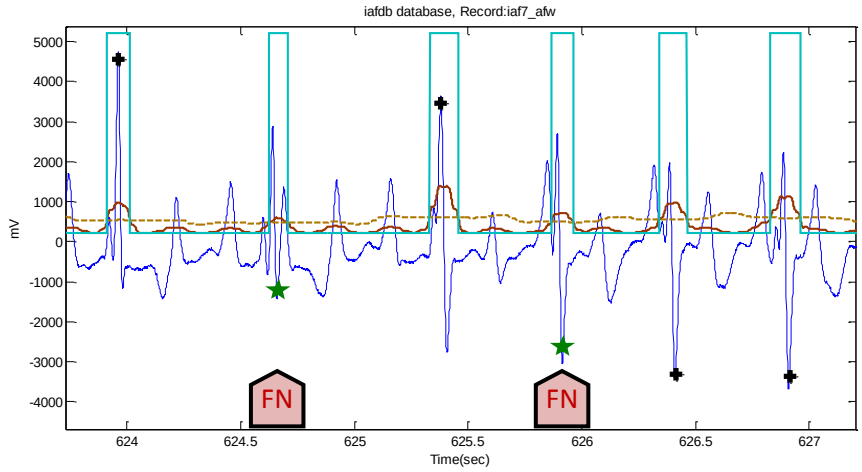

Figure 13 Isolated QRS-like artifacts in Record iaf7_afw-IAFDB. The dotted line is the first moving average MA_{QRS} and the solid line is the second moving average $MA_{OneBeat}$. The arrows point to FNs. '+' represents a successful detection produced by the proposed algorithm, where the green star represents FN.

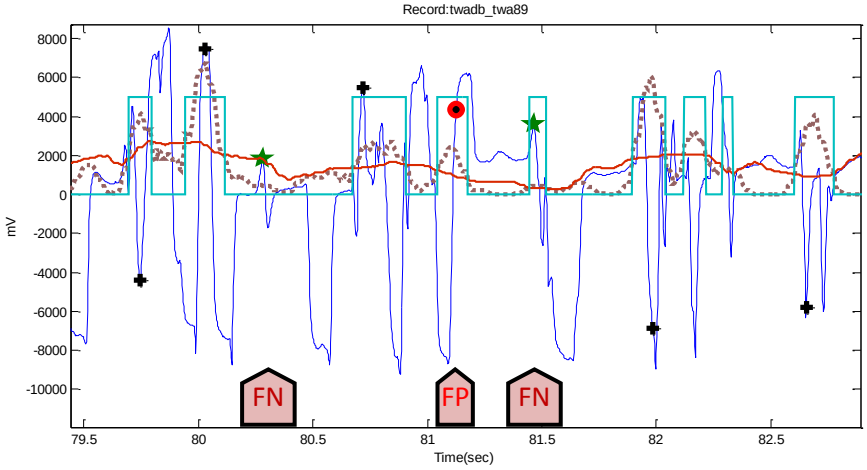

Figure 14 Low-amplitude QRS complexes lie between T wave alternans in Record twa89-TWADB. The dotted line is the first moving average MA_{QRS} and the solid line is the second moving average $MA_{OneBeat}$. The arrows point to FNs and FP. '+' represents a successful detection produced by the proposed algorithm, and the red circle represents FP, while the green star represents FN.

Figure 13 shows how the isolated QRS-like artifacts caused FNs in Record iaf7_afw from the IAF database, scoring the highest number of FNs, 80 FNs out of a total of 83. On the other hand, the number of FPs was the highest, 250 out of a total 419 FPs, in Record iaf5_afw, which contains wide U waves similar to the example presented in Figure 12.

It can be seen in Figure 14, because of the T wave alternans and low-amplitude QRS complexes, detecting R peaks is challenging. The performance of the detector on the TWA database incurred 156 FPs and 230 FNs. The first FN (at left) occurred because the moving average could not generate blocks of interest; however, the second FN (at right) happened given the fact that it has been demarcated (cf. Figure 14). The duration of the block (second FN at right) is below the optimized duration of QRS complex W_1, and is thus rejected causing FN, while the FP arises due to the existence of noisy T wave alternans.

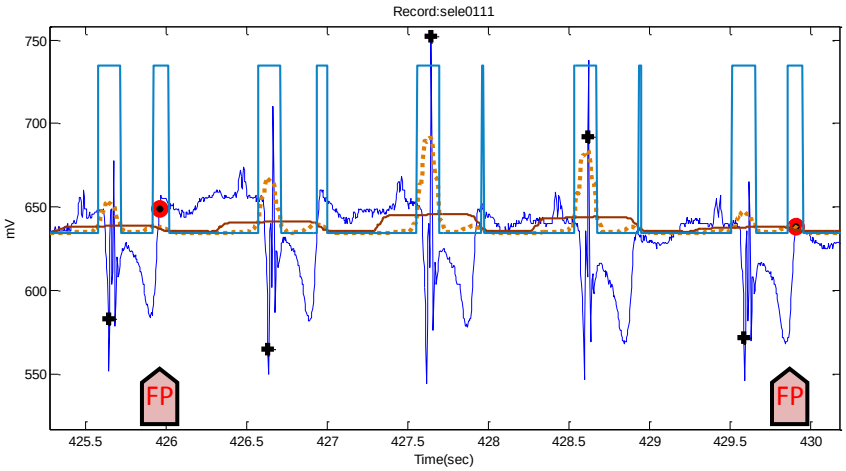

Figure 15 Steeply upward-sloping T waves in Record sele0111-QTDB. The dotted line is the first moving average MA_{QRS} and the solid line is the second moving average $MA_{OneBeat}$. The arrows point to FPs. '+' represents a successful detection produced by the proposed algorithm, and the red circle represents FP.

Analyzing the performance of NSTDB is quite confusing, perhaps because the annotations are not completely correct and certainly need modification. However, the detector ran over the dataset as it is and incurred 2844 FPs and 1199 FNs overall.

Regarding the ST database, FPs and FNs were 131 and 33 in total, respectively. The highest number of FPs occurred in Record 305-STDB due to large T waves, while the inverted polarity of QRS complexes caused the large number of FNs.

The detectors obtained a total of 305 FPs and 3 FNs over the QT database. The FPs are mainly caused by the steeply upward-sloping T waves (cf. Figure 15).

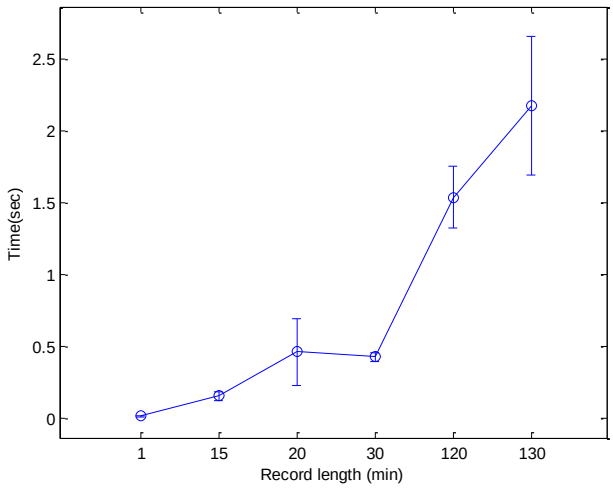

Figure 16 Processing time of ECG recordings. The 11 datasets contain various ECG recording lengths from one minute to 130 minutes. The average processing time of one-minute ECG record is 8.9 milliseconds, while for 130 minutes of recording the average processing time is 2.2 seconds.

Processing Time

The processing time of a detector developed is rarely discussed in literature. However, recently, Yeh and Wang considered the detector's speed in their study [57]. With 1.6 GHz AMD CPU, their Matlab-programmed detector takes 22–30 seconds for handling 10-minute-long ECG records. Moreover, they found that their algorithm was faster than Pan-Tomkins' algorithm and Wavelet transform methods.

In this study, the proposed detector was implemented in Matlab 7.11 (R2010b) on Intel i5 CPU 2.27 GHz. Perhaps it is misleading to suggest that mentioning the average speed of the proposed detector, over a certain time length of ECG signal, would provide a comparative result. This is because the processing time depends on the number of beats within each ECG recording, not on the record length.

As the 11 databases contain different recording lengths, a categorization by recording length is needed to evaluate the detector's speed properly.

It can be seen in Figure 16 that the speed of the detector varies inconsistently across all recoding-length categories. The speed measured in seconds, while the recording-length category was in minutes.

The number of beats of the 30-minute recordings category was relatively consistent—with a mean ± SD, number of beats 2291 ± 448— over all records of this category. The same holds for 1-minute and 15-minute recording categories.

On the contrary, the 130-min beats average was 10,171 with an SD of 2,600 beats, thus the processing time depends on the number of beats rather than the recording length. For example, Record 16272-NSRDB contains 7,988 beats, and the detector took 1.5 seconds to process it, while it took 3.5 seconds to process 14,875 beats in Record 19830-NSRDB.

In general, without taking the number of beats into consideration, the speed of the proposed detector is faster than Yeh-Wang's detector [57]. The suggested detector handles 15-minute recordings in about 0.15 seconds, while Yeh-Wang's detector takes 22–30 seconds to handle 10-minute ECG recordings.

Conclusion

The accurate detection of QRS complexes is important for ECG signal analysis. The performance of the optimized knowledge-based detector is promising. It has been tested on different databases that contain unusual noise, QRS, T waves and U waves morphologies.

The extensive use of the MIT-BIH Database as a testing database can hide an overtuning of the detector parameters to fit this particular database. Consequently, the validation of the same detector on a second dataset without any later parameter tuning can help to obtain more reliable performance results. After applying the same algorithm on other databases, high detection rates were obtained on the QT database, NSR, TWA, IAF, ST, SV, AFT, FANTASIA, NST and ICART databases.

Interestingly, the detector's speed over 130-minute recordings is about 2.2 seconds, thus the proposed detector is the most promising tool to process large-recorded ECG signals. Furthermore, its simplicity makes it an ideal algorithm for mobile-phone applications and battery-driven ECG signal devices.

The proposed detector may have several interesting applications in online analysis of cardiac data collected by the smallest long-term recording devices that have been studied in the form of necklaces and smart electrodes.

The assessment of the QRS detector has been reliably done over the existing standard databases. Moreover, the number of annotated beats used in testing the new algorithm is considered sufficient as it is tested on a good representation of the possible morphologies found in ECG signals.

Acknowledgement

The author would like to thank Dr Gari Clifford for helpful discussions. Mohamed Elgendi would like to gratefully acknowledge the Australian government and Charles Darwin University whose generous scholarships facilitated this research.

References

1. World Health Organization (2011) Global status report on noncommunicable disaeses 2010. Geneva.
2. Dilaveris PE, Gialafos EJ, Sideris SK, Theopistou AM, Andrikopoulos GK, et al. (1998) Simple electrocardiographic markers for the prediction of paroxysmal idiopathic atrial fibrillation. American Heart Journal 135: 733-738.
3. Ren-Guey L, Yih-Chien C, Chun-Chieh H, Chwan-Lu T (2007) A Mobile Care System With Alert Mechanism. Information Technology in Biomedicine, IEEE Transactions on 11: 507-517.
4. Rasid MFA, Woodward B (2005) Bluetooth telemedicine Processor for multichannel biomedical signal transmission via mobile cellular networks. Information Technology in Biomedicine, IEEE Transactions on 9: 35-43.
5. Wen C, Yeh M-F, Chang K-C, Lee R-G (2008) Real-time ECG telemonitoring system design with mobile phone platform. Measurement 41: 463-470.
6. Oresko J (2010) Portable heart attack warning system by monitoring the ST segment via smartphone electrocardiogram processing: University of Pittsburgh.
7. Muñoz-Ramos O, Starostenko O, Alarcon-Aquino V, Cruz-Perez C (2013) Real-Time System for Monitoring and Analyzing Electrocardiogram on Cell Phone. In: Elleithy K, Sobh T, editors. Innovations and Advances in Computer, Information, Systems Sciences, and Engineering: Springer New York. pp. 327-338.
8. Gradl S, Kugler P, Lohmuller C, Eskofier B (2012) Real-time ECG monitoring and arrhythmia detection using Android-based mobile devices. the 2012 Annual International Conference of the IEEE Engineering in Medicine and Biology Society (EMBC). pp. 2452-2455.
9. Hii P-C, Chung W-Y (2011) A Comprehensive Ubiquitous Healthcare Solution on an Android™ Mobile Device. Sensors 11: 6799-6815.
10. Jasemian Y, Arendt-Nielsen L (2005) Evaluation of a realtime, remote monitoring telemedicine system using the Bluetooth protocol and a mobile phone network. Journal of Telemedicine and Telecare 11: 256-260.
11. Jurik AD, Weaver AC (2008) Remote Medical Monitoring. Computer 41: 96-99.
12. Arzeno N, Deng Z, Poon C (2008) Analysis of First-Derivative Based QRS Detection Algorithms. IEEE Transactions on Biomedical Engineering 55: 478-484.
13. Paoletti M, Marchesi C (2006) Discovering dangerous patterns in long-term ambulatory ECG recordings using a fast QRS detection algorithm and explorative data analysis. Computer Methods and Programs in Biomedicine 82: 20-30.
14. Sufi F, Fang Q, Cosic I (2007) ECG R-R Peak Detection on Mobile Phones. the 29th Annual International Conference of the IEEEEngineering in Medicine and Biology Society. pp. 3697-3700.
15. Martín-Clemente R, Camargo-Olivares JL, Hornillo-Mellado S, Elena M, Roman I (2011) Fast Technique for Noninvasive Fetal ECG Extraction. IEEE Transactions on Biomedical Engineering 58: 227-230.
16. Zhang CF, Tae-Wuk B (2012) VLSI Friendly ECG QRS Complex Detector for Body Sensor Networks. IEEE Journal on Emerging and Selected Topics in Circuits and Systems 2: 52-59.
17. Pan J, Tompkins WJ (1985) A Real-Time QRS Detection Algorithm. IEEE Transactions on Biomedical Engineering 32: 230-236.
18. Goldberger AL, Amaral LAN, Glass L, Hausdorff JM, Ivanov PC, et al. (2000) PhysioBank, PhysioToolkit, and PhysioNet: Components of a New Research Resource for Complex Physiologic Signals. Circulation 101: e215-e220.
19. Moody GB, Mark RG (2001) The impact of the MIT-BIH Arrhythmia Database. IEEE Engineering in Medicine and Biology Magazine 20: 45-50.

20. Laguna P, Mark RG, Goldberg A, Moody GB (1997) A database for evaluation of algorithms for measurement of QT and other waveform intervals in the ECG. Computers in Cardiology. pp. 673-676.
21. Moody GB (2008) The PhysioNet / Computers in Cardiology Challenge 2008: T-Wave Alternans. Computers in Cardiology. pp. 505-508.
22. Albrecht P (1983) S-T segment characterization for long-term automated ECG analysis [M.S. thesis]: MIT Dept. of Electrical Engineering and Computer Science.
23. Greenwald S (1990) Improved detection and classification of arrhythmias in noise-corrupted electrocardiograms using contextual information [Ph.D. thesis]: Harvard-MIT Division of Health Sciences and Technology.
24. Moody GB (2004) Spontaneous termination of atrial fibrillation: a challenge from physionet and computers in cardiology 2004. Computers in Cardiology. pp. 101-104.
25. Iyengar N, Peng CK, Morin R, Goldberger AL, Lipsitz LA (1996) Age-related alterations in the fractal scaling of cardiac interbeat interval dynamics. American Journal of Physiology - Regulatory, Integrative and Comparative Physiology 271: R1078-R1084.
26. Moody GB, Muldrow WE, Mark RG (1984) A noise stress test for arrhythmia detectors. Computers in Cardiology. pp. 381-384.
27. Friesen GM, Jannett TC, Jadallah MA, Yates SL, Quint SR, et al. (1990) A comparison of the noise sensitivity of nine QRS detection algorithms. IEEE Transactions on Biomedical Engineering 37: 85-98.
28. Braunwald E, Zipes D, Libby P, Bonow R (2004) Braunwald's Heart Disease: A Textbook of Cardiovascular Medicine. Philadelphia: Saunders.
29. Clifford GD, Azuaje F, McSharry P (2006) Advanced Methods And Tools for ECG Data Analysis. Artech House Publishers 1st edition.
30. Oppenheim A, Shafer R (1989) Discrete-time Signal Processing. NJ: Prentice Hall. 411-425 p.
31. Thakor NV, Webster JG, Tompkins WJ (1983) Optimal QRS detector. Medical and Biological Engineering 21: 343-350.
32. Chen HC, Chen SW. A moving average based filtering system with its application to real-time QRS detection; 2003. pp. 585-588.
33. Firbank M, Coulthard A, Harrison R, Williams E (1999) A comparison of two methods for measuring the signal to noise ratio on MR images. Physics in Medicine and Biology 44: 261-264.
34. Adnane M, Jiang Z, Choi S (2009) Development of QRS detection algorithm designed for wearable cardiorespiratory system. Computer Methods and Programs in Biomedicine 93: 20-31.
35. Ghaffari A, H. Golbayani, M. Ghasemi (2008) A new mathematical based QRS detector using continuous wavelet transform. Computers and Electrical Engineering 34.
36. Huabin Z, Jiankang W (2008) Real-time QRS detection method. The 10th International Conference on e-health Networking, Applications and Services. pp. 169-170.
37. Fard P, Moradi M, Tajvidi M (2007) A novel approach in R peak detection using Hybrid Complex Wavelet (HCW). International Journal of Cardiology 124: 250-253.
38. Darrington J (2006) Towards real time QRS detection: A fast method using minimal pre-processing. Biomedical Signal Processing and Control 1: 169-176.
39. Chen S, Chen HC, Chan HL (2006) A real-time QRS detection method based on moving-averaging incorporating with wavelet denoising. Computer Methods and Programs in Biomedicine 82: 187-195.
40. Martinez JP, Almeida R, Olmos S, Rocha AP, Laguna P (2004) A wavelet-based ECG delineator: evaluation on standard databases. IEEE Transactions on Biomedical Engineering 51: 570-581.
41. Hamilton P (2002) Open source ECG analysis. Computers in Cardiology. pp. 101-104.
42. Lee J, Jeong K, Yoon J, Lee M (1996) A simple real-time QRS detection algorithm. the 18th Annual International Conference of the IEEE Engineering in Medicine and Biology Society. pp. 1396-1398.
43. Afonso VX, Tompkins WJ, Nguyen TQ, Luo S (1996) Filter bank-based ECG beat detection. the 18th Annual International Conference of the IEEE Engineering in Medicine and Biology Society. pp. 1037-1038 vol.1033.
44. Li C, Zheng C, Tai C (1995) Detection of ECG characteristic points using wavelet transforms. IEEE Transactions on Biomedical Engineering 42: 21-28.

45. Hamilton PS, Tompkins WJ (1986) Quantitative investigation of QRS detection rules using the MIT/BIH arrhythmiac database. IEEE Transactions in Biomedical Engineering 33: 1157-1165.
46. Benitez DS, Gaydecki PA, Zaidi A, Fitzpatrick AP (2000) A new QRS detection algorithm based on the Hilbert transform. Computers in Cardiology. pp. 379-382.
47. Xue Q, Hu YH, Tompkins WJ (1992) Neural-network-based adaptive matched filtering for QRS detection. IEEE Transactions on Biomedical Engineering 39: 317-329.
48. MIT-BIH Arrhythmia Database. wwwphysionetorg.
49. Li C Z, C TC (1995) Detection of ECG characteristic points using wavelet transforms. IEEE Trans on Biomed Eng: 21-28.
50. Moraes JCTB, Freitas MM, Vilani FN, Costa EV (2002) A QRS complex detection algorithm using electrocardiogram leads. Computers in Cardiology. pp. 205-208.
51. Engelse W, Zeelenberg C (1979) A single scan algorithm for QRS detection and feature extraction. Computers in Cardiology. pp. 37-42.
52. Ligtenberg A, Kunt M (1983) A robust-digital QRS detection algorithm for arrhythmia monitoring. Computers and Biomed Res: 273-286.
53. Alvarado C, Arregui J, Ramos J, Pallas-Areny R (2005) Automatic detection of ECG ventricular activity waves using continuous spline wavelet transform. the 2nd International Conference on Electrical and Electronics Engineering. pp. 189-192.
54. Fei Zhang, Yong Lian (2007) Novel QRS Detection by CWT for ECG Sensor. IEEE Biomedical Circuits and Systems Conference (BIOCAS 2007) 211-214.
55. Sahambi JS, Tandon SN, Bhatt RKP (1997) Using wavelet transforms for ECG characterization. An on-line digital signal processing system. IEEE Engineering in Medicine and Biology Magazine 16: 77-83.
56. Mahmoodabadi SZ, Ahmadian A, Abolhasani MD (2005) ECG Feature Extraction Using Daubechies Wavelets. The Fifth IASTED International Conference on Visualization, Imaging, and Image Processing.
57. Yeh Y-C, Wang W-J (2008) QRS complexes detection for ECG signal: The Difference Operation Method. Computer Methods and Programs in Biomedicine 91: 245-254.